ARMY RESEARCH LABORATORY

Microfabricated Amorphous Silicon Nanopillars on an Ultrasmooth 500-nm-thick Titanium Adhesion Layer

by Collin R. Becker, Kenneth E. Strawhecker, Jonathan P. Ligda, and Cynthia A. Lundgren

ARL-TR-6209 **September 2012**

NOTICES

Disclaimers

The findings in this report are not to be construed as an official Department of the Army position unless so designated by other authorized documents.

Citation of manufacturer's or trade names does not constitute an official endorsement or approval of the use thereof.

Destroy this report when it is no longer needed. Do not return it to the originator.

Army Research Laboratory
Adelphi, MD 20783-1197

ARL-TR-6209 **September 2012**

Microfabricated Amorphous Silicon Nanopillars on an Ultrasmooth 500-nm-thick Titanium Adhesion Layer

Collin R. Becker, Kenneth E. Strawhecker, Jonathan P. Ligda, and Cynthia A. Lundgren
Sensors and Electron Devices Directorate, ARL

REPORT DOCUMENTATION PAGE	Form Approved OMB No. 0704-0188

PLEASE DO NOT RETURN YOUR FORM TO THE ABOVE ADDRESS.

1. REPORT DATE *(DD-MM-YYYY)*	2. REPORT TYPE	3. DATES COVERED (From - To)
September 2012	Final	

4. TITLE AND SUBTITLE

Microfabricated Amorphous Silicon Nanopillars on an Ultrasmooth 500-nm-thick Titanium Adhesion Layer

5a. CONTRACT NUMBER

5b. GRANT NUMBER

5c. PROGRAM ELEMENT NUMBER

6. AUTHOR(S)

Collin R. Becker, Kenneth E. Strawhecker, Jonathan P. Ligda, and Cynthia A. Lundgren

5d. PROJECT NUMBER

5e. TASK NUMBER

5f. WORK UNIT NUMBER

7. PERFORMING ORGANIZATION NAME(S) AND ADDRESS(ES)

U.S. Army Research Laboratory
ATTN: RDRL-SED-C
2800 Powder Mill Road
Adelphi, MD 20783-1197

8. PERFORMING ORGANIZATION REPORT NUMBER

ARL-TR-6209

9. SPONSORING/MONITORING AGENCY NAME(S) AND ADDRESS(ES)

10. SPONSOR/MONITOR'S ACRONYM(S)

11. SPONSOR/MONITOR'S REPORT NUMBER(S)

12. DISTRIBUTION/AVAILABILITY STATEMENT

Approved for public release; distribution unlimited.

13. SUPPLEMENTARY NOTES

14. ABSTRACT

Amorphous silicon (Si) nanopillars are fabricated using electron beam lithography for a liftoff process. The nanopillars are fabricated on an ultrasmooth, 6.5-nm root mean square (RMS) roughness, 500-nm-thick titanium (Ti) layer using electron beam evaporation. Pillars ranging from 100–1000 nm in diameter and approximately 200 nm in height are fabricated. Atomic force microscopy (AFM) and scanning electron microscope (SEM) images, including those collected by focused ion beam (FIB) milling, are presented to analyze the shape of the pillars and roughness of the Ti film. The smoother the Ti/Si interface, the more robust the adhesion of Si to Ti becomes.

15. SUBJECT TERMS

Silicon, electron beam lithography, nanopillar, nanowire

16. SECURITY CLASSIFICATION OF:			17. LIMITATION OF ABSTRACT	18. NUMBER OF PAGES	19a. NAME OF RESPONSIBLE PERSON
a. REPORT	b. ABSTRACT	c. THIS PAGE			Collin R. Becker
Unclassified	Unclassified	Unclassified	UU	24	19b. TELEPHONE NUMBER (*Include area code*) (301) 394-0476

Standard Form 298 (Rev. 8/98)
Prescribed by ANSI Std. Z39.18

Contents

List of Figures

List of Tables

Acknowledgments

We would like to thank Dr. Madhu Roy and Dr. Rob Burke for discussion with electron beam lithography and acknowledge the U.S. Army Research Laboratory for funding.

INTENTIONALLY LEFT BLANK.

1. Introduction

Silicon (Si) is viewed as one of the most promising materials to improve the energy capacity of lithium-ion batteries. Work by many groups demonstrates that nanoscale Si offers dramatic improvements in cycle life compared to bulk-scale Si (*1, 2*). The reasons for this improvement have been explored from many angles, but more work is needed to clarify the precise reasons for this improvement. Specifically, studies of Si nanostructures anchored to a metal current collector such as copper or titanium (Ti) need further refinement and study to explore volume change and interface effects from the substrate.

Here, methods to produce precision amorphous Si nanopillars on a Ti substrate using microfabrication techniques including electron beam lithography and liftoff methods are described. The method is somewhat unusual in that the adhesion layer, Ti, is exposed to air prior to Si deposition and is quite thick, 500 nm. A similar approach has been used by other research groups (*3*). Presented here, using atomic force microscopy (AFM), Raman spectroscopy, focused ion beam (FIB), and scanning electron microscopy (SEM), is a detailed investigation of the size and shape, phase (amorphous or crystalline), and Si/Ti interface of the pillars.

2. Experimental

2.1 Titanium Deposition

We used Si wafers with a resistivity of 1–20 ohm-cm or 0.01–0.02 ohm-cm (the resistivity is chosen for particular end applications). Ti of 99.995% purity was deposited using an Evatek BAK 641 electron beam evaporator at either 0.2 or 0.05 nm/s operating at 1.9 x 10^{-6} mbar initial background pressure. The thickness was monitored by quartz crystal.

2.2 Nanopattern Fabrication

After Ti deposition, the wafers were pretreated with 10 ml of liquid hexamethyldisilazane (HMDS) to promote adhesion by photoresist. The HMDS was removed by rotating the wafer at 2000 rpm for 40 s and then heating on a hot plate for 60 s at 110 °C. Next, approximately 5 ml of positive electron beam photoresist (ZEP 520A) was deposited on the wafer. The wafer was spun at 2000 rpm for 60 s and then baked on a hot plate for 180 s at 175 °C. The thickness of the photoresist was 389 nm as confirmed by stylus profilometry (Tencor).

The desired nanopillar pattern was transferred to the resist using electron-beam lithography (Vistec EBPG5000+ES). The pattern was generated using a beam at a 100-kV, 10-pA current

and with a 300-μCcm^{-2} dose. Additionally, square Si pads used as guides when locating pillars for images were patterned using a 50-pA beam and 300-μCcm^{-2} dose. The write time for four samples per wafer composed of 1x10^6 pillars/sample was approximately 50 min. The resist was then developed for 90 s at 21 °C in xylenes and then was rinsed for 30 s in methyl isobutyl ketone (MIBK).

2.3 Silicon Deposition and Liftoff

Prior to deposition, a 5-min descum operation using an Anatech barrel asher was performed. The power was tuned to 200 W and the gas flow was 400 sccm. After this descum, the resist thickness was 368 nm. Again using electron beam evaporation (Evatek BAK 641), Si (99.999%) was deposited at a rate of 0.2 nm/s. The thickness was monitored by quartz crystal. For liftoff, the wafer was immersed in acetone until most of the photoresist/Si had been removed. The wafers were then rinsed with acetone, methanol, isopropyl alcohol (IPA), deionized (DI) water, and transferred without drying to a Microposit 1165 photoresist remover and held at 80 °C for 2 h. The wafers were then rinsed in DI water and dried with flowing nitrogen. As a final step, a Metroline oxygen plasma etcher operating at 400 W and 500 sccm was used to help remove photoresist debris.

2.4 Characterization

AFM (either a Veeco Dimension 3100 or Agilent 5500) was used to measure heights and diameters of the pillars and roughness of the substrate. SEM (FEI environmental SEM) was used to investigate morphology of the pillars and a FIB microscope (FEI) was used to analyze the interface of the pillars. A Renishaw Raman InVia system with a 514 nm wavelength laser was used for Si phase analysis.

3. Results and Discussion

Figure 1a and b show SEM cross sections of the 0.2 and 0.05 nm/s Ti films on Si, respectively. The films are measured to be within ±20 nm of the 500-nm target thickness. The 0.2-nm/s film shows large columnar grains while the 0.05-nm/s film has a microstructure with smaller grains.

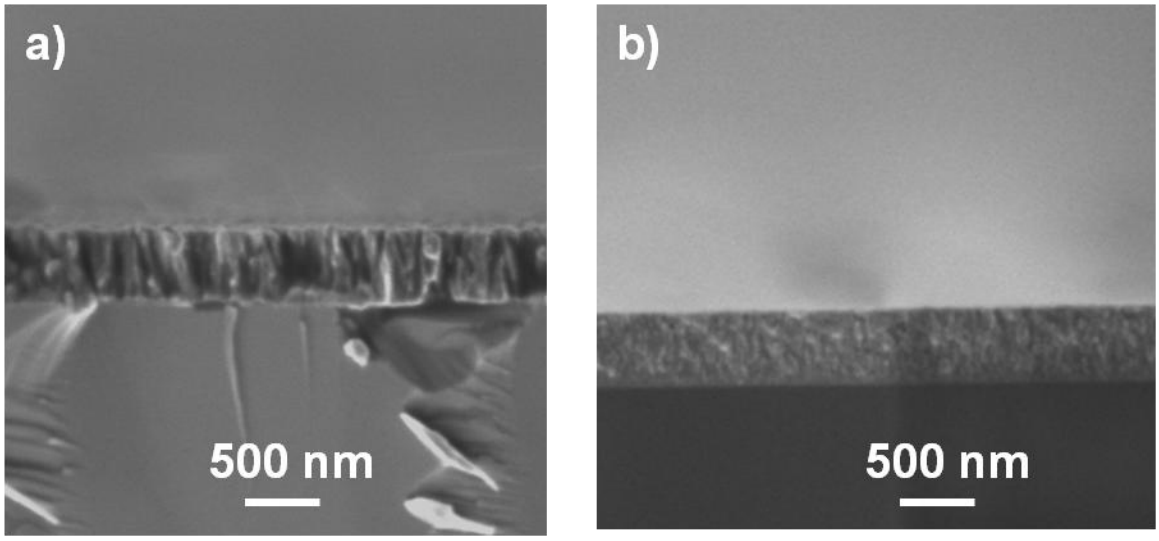

Figure 1. The 500-nm-thick Ti films deposited at (a) 0.2 nm/s and (b) 0.05 nm/s.

Figure 2a and c show the array of pillars and the 100-nm pillar, respectively. The Si pillars in this case are deposited on 500 nm of Ti deposited at a rate of 0.2 nm/s. The Ti grains are large and the film surface is rough. On the contrary, the array of pillars and the 100-nm pillar shown in figure 2b and d, respectively, are deposited on 500 nm of Ti deposited at a rate of 0.05 nm/s. The Ti grains are much smaller and the surface is quite smooth. These results are similar to reference 4, where smaller grains and a smoother surface results from a lower flux of Ti atoms to the surface. It is expected that at slower deposition rates and decreased flux of Ti atoms to the surface, grain growth and nucleation slows leading to smaller grains and a smoother surface. While a thorough study was not carried out, appendix A shows SEM results from a sputtered Ti film with a high flux of Ti atoms and shows large grains and a rough surface.

In figure 2b, some residue can be seen near the 1000-nm pillars on the top row of the image.

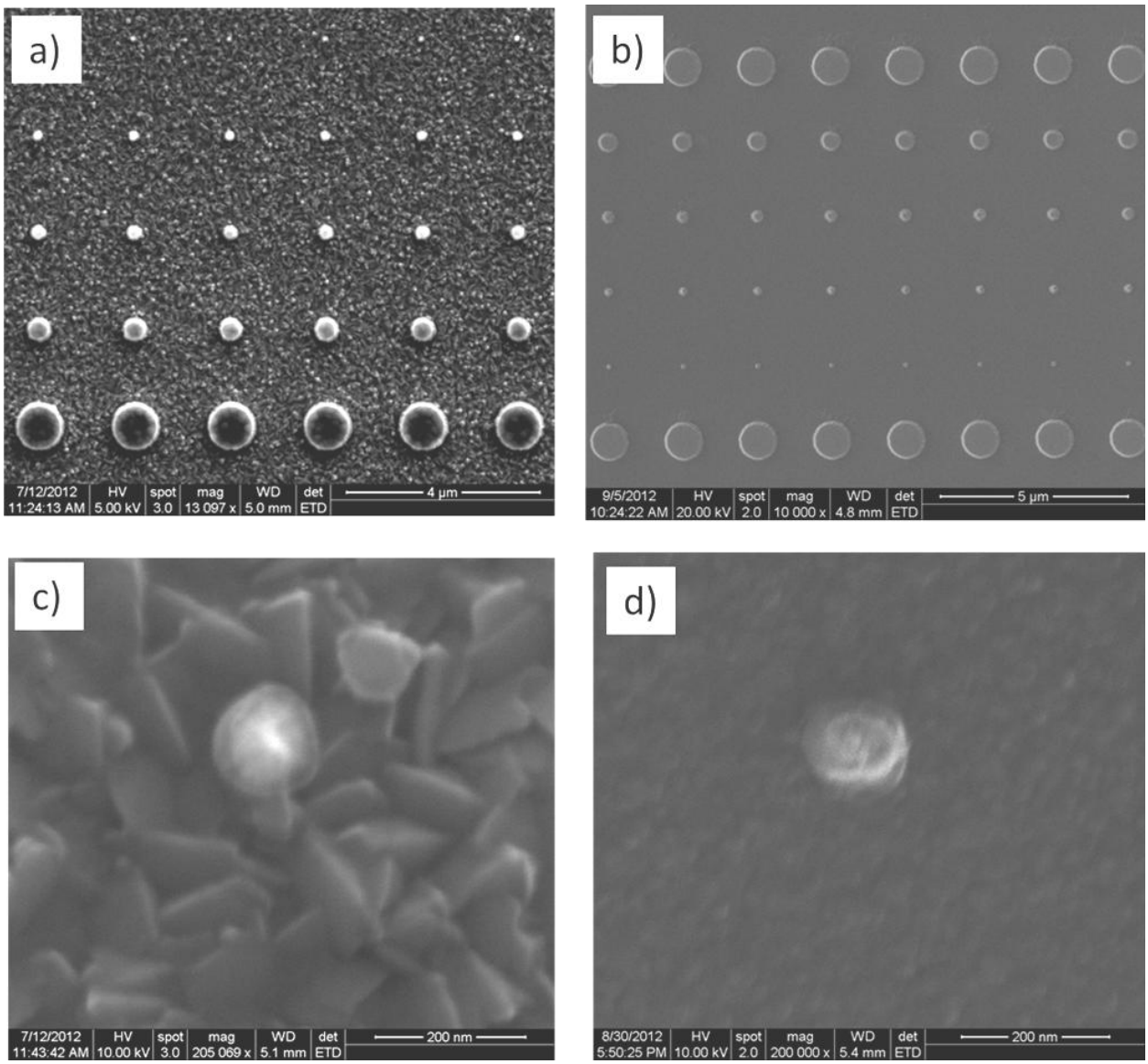

Figure 2. (a) Si nanopillars deposited on 500-nm-thick "rough" Ti, 0.2 nm/s deposition rate; (b) Si nanopillars deposited on 500-nm-thick "smooth" Ti, 0.05 nm/s deposition rate; (c) 100-nm-diameter pillar on the "rough" Ti; and (d) 100-nm pillar on the "smooth" Ti.

Initially, this was suspected to be photoresist residue and an oxygen plasma treatment (ash) was performed as an attempt to remove the photoresist. Figure 3a and b shows an AFM image of the pillars pre- and post-ash.

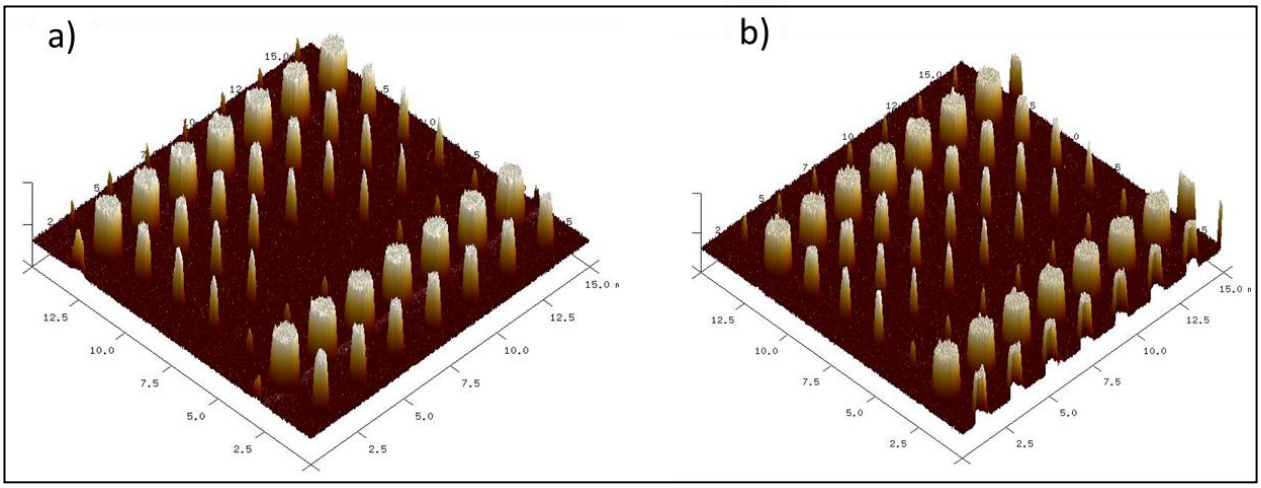

Figure 3. AFM images of Si nanopillars (a) pre- and (b) post-oxygen plasma ash treatment.

The ash treatment does not appear to degrade the substrate or pillars since the heights remain similar. However, the residue is still present and the exact cause and composition of this residue is being investigated. It was found that with ultrasonic treatment during the lift-off process, the residue was not as prevalent; however, the ultrasonic treatment had a tendency to delaminate some pillars, as seen in figure 1a, and is not a preferred technique. This result seems to indicate the residue is redeposition of either photoresist or Si during the liftoff process.

Tables 1 and 2 present the heights and diameters of the pillars pre- and post-ash. The averages are computed for 5–7 pillars and do not appear to be drastically different after the ash. Some of the difference arises from the inability to examine the exact same pillars after the ash or from slight tip degradation during scanning.

Table 1. Average height of Si nanopillars pre oxygen plasma treatment.

Pre Oxygen Plasma Treatment	
Designed Pillar Diameter (nm)	Average Height (nm)
1000	231 +/- 2
500	240 +/- 2
300	255 +/- 10
200	255 +/- 6
100	117 +/- 6

Table 2. Average height of Si nanopillars post oxygen plasma treatment.

Post Oxygen Plasma Treatment	
Designed Pillar Diameter (nm)	Average Height (nm)
1000	219 +/- 1
500	229 +/- 2
300	249 +/- 2
200	251 +/- 5
100	139 +/- 13

Table 3 indicates the diameter of the pillars on the smooth Ti substrate. AFM is known to be extremely accurate in the Z-direction, but can have a tip broadening effect in the x,y direction. Here it is shown that the AFM overestimates the diameter of the pillar since the pillar diameter is larger at full width at half maximum (FWHM) than even SEM shows for the base of the pillar. AFM can give the approximate slope of the sidewalls of the pillars though, and it is found to be around 60°. This agrees closely to the SEM image shown in appendix B, which has a measured angle near 51°. In the future, a more vertical sidewall is likely to be desired, which may be found by heat treatment of the photoresist (*5*) or perhaps working with poly(methyl methacrylate) (PMMA) rather than ZEP electron beam photoresists.

Table 3. Comparison of designed pillar diameter with diameters measured by AFM and SEM.

Designed Pillar Diameter (nm)	AFM Actual Diameter, FWHM (nm)	SEM Actual Diameter, Base (nm)
1000	1085 +/- 15	1060 +/- 32
500	569 +/- 16	531 +/- 18
300	387 +/- 8	363 +/- 12
200	258 +/- 20	261+/- 6
100	234 +/- 21	153 +/- 19

Figure 4 shows AFM images of the Ti substrate of the rough (0.2 nm/s) and smooth (0.05 nm/s) Ti in figure 4a and b, respectively. The root mean square (RMS) of the rough Ti is 29.9 nm and the RMS of the smooth Ti is 6.5 nm. Additionally the grains are much smaller in the smooth Ti. Figure 4a and b are tilted at a slightly different angle to best show the grain morphology, but the reader should note that both are from a 1.5x1.5 μm area so the grains are indeed considerably larger for the rough Ti.

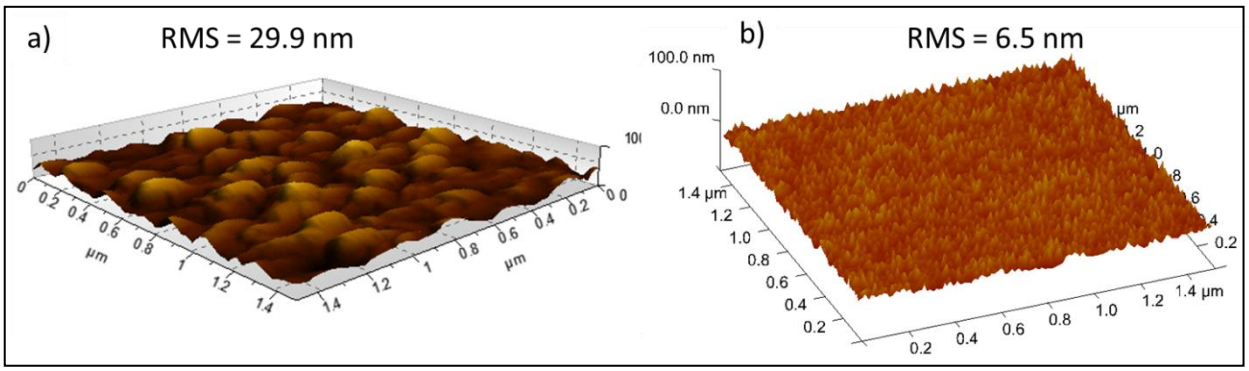

Figure 4. AFM images of 500 nm thick Ti deposited at (a) 0.2 nm/s and (b) 0.05 nm/s.

The rough Ti is indeed problematic as it leads to very poor adhesion of the Si pillars, as shown in figure 5.

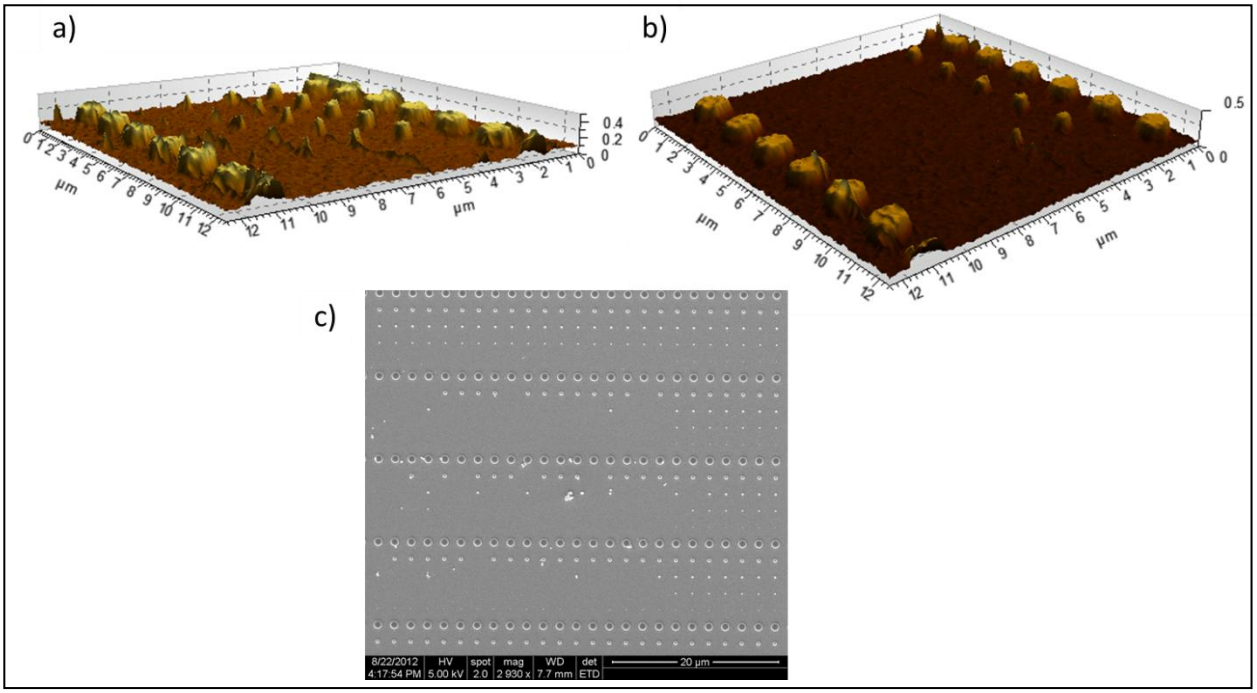

Figure 5. AFM images of Si pillars on "rough" Ti with poor adhesion on (a) the initial scan, (b) the second scan, and (c) is an SEM image showing a large region of missing pillars as a result of AFM interaction.

Figure 5a shows an initial scan of a region of pillars. Figure 5b shows the second scan of the region and many pillars are missing as the tip passed over the sample initially. Figure 5c shows an SEM picture of the region after AFM imaging and it is obvious the pillars have been removed from the surface.

FIB milling of the samples was carried out to observe the interface of the Ti and Si for the 0.05-nm/s Ti. Figure 6a shows the as-fabricated 1000-nm-diameter pillar, figure 6b shows the pillars where FIB was used, and figure 6c shows the cross section of the 1000-nm pillar.

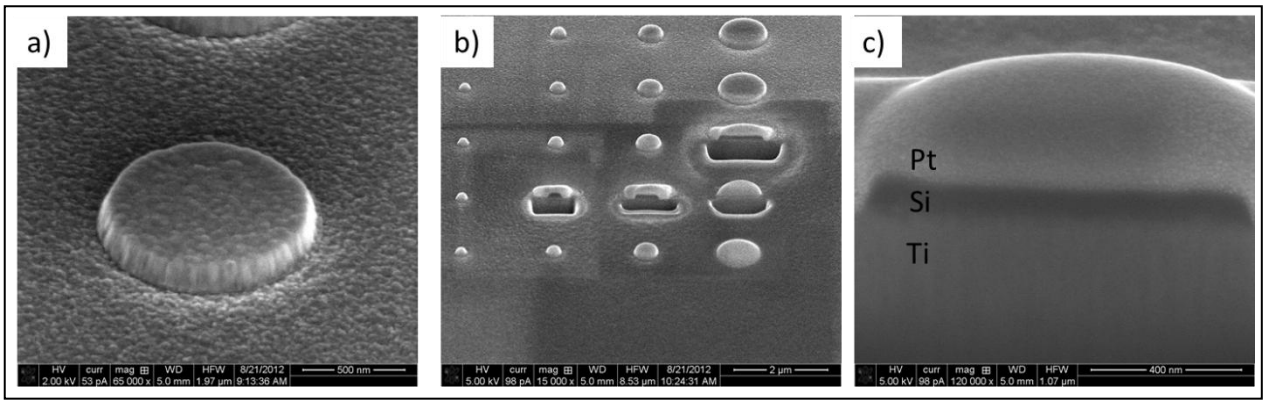

Figure 6. (a) An SEM image at oblique angle of the 1000-nm pillar, (b) an SEM image of pillars analyzed with FIB, and (c) a close up SEM image after FIB milling of the 1000-nm pillar.

A platinum (Pt) mask is deposited in the FIB to reduce damage caused by milling. The Si/Ti interface is observed to be uniform and smooth without gaps. The Si is also seen to be smooth and dense.

Lastly, to confirm the pillars are amorphous, Raman spectroscopy with a 514-nm laser was used. Figure 7 shows a Raman spectrum from the Si pillars and the peak centered near 480 cm^{-1} indicates the pillars are amorphous Si (*6*).

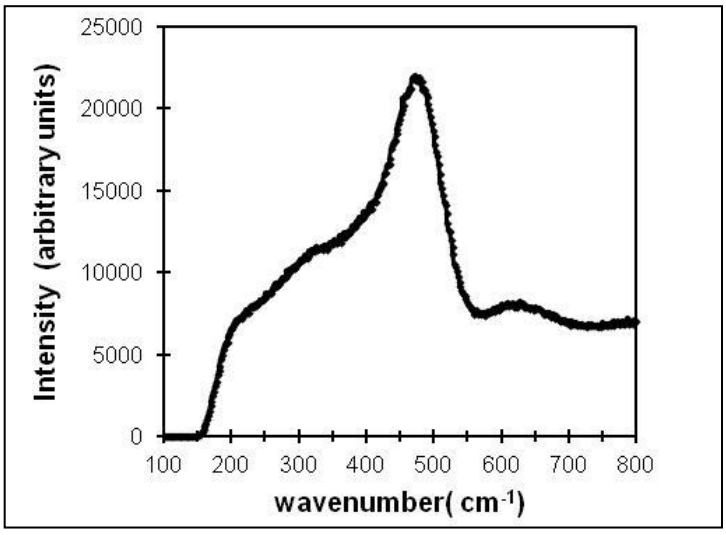

Figure 7. Raman spectrum of Si nanopillars.

4. Conclusion

Amorphous Si nanopillars are fabricated with a lift-off method using electron beam lithography. The pillars are deposited by electron beam evaporation on top of a Ti film. It is imperative that a smooth Ti film is grown for this method to yield Si pillars with good adhesion to the Ti. Using a slow deposition rate (0.05 nm/s) of Ti can achieve smooth (6.5 nm RMS) films that are 500 nm thick.

5. References

1. Chan, C. K., et al. High-performance Lithium Battery Anodes using Silicon Nanowires. *Nature Nanotechnology* **2008**, *3* (1), 31–35.

2. Szczech, J. R.; Jin, S. Nanostructured Silicon for High Capacity Lithium Battery Anodes. *Energy & Environmental Science* **2011**, *4* (1), 56–72.

3. Soni, S. K., et al. Stress Mitigation During the Lithiation of Patterned Amorphous Si Islands. *Journal of the Electrochemical Society* **2012**, *159* (1), A38–A43.

4. Cai, K. Y., et al. Surface Structure and Composition of Flat Titanium Thin Flms as a Function of Film Thickness and Evaporation Rate. *Applied Surface Science* **2005**, *250* (1–4), 252–267.

5. Meyer, D. J., et al. *40 nm T-Gate Process Devlopment Using ZEP Reflow*. in *CS MANTECH Conference*, Boston, 2012.

6. Brodsky, M. H.; Cardona, M.; Cuomo, J. J. Infrared and Raman-spectra of Silicon-hydrogen Bonds in Amorphous Silicon Prepared by Glow-discharge and Sputtering. *Physical Review B* **1977**, *16* (8), 3556–3571.

Appendix A. SEM Analysis of Sputtered Ti Film

Ti films were also obtained by sputtering using a CLC 200 Unaxis Clusterline DC magnetron Sputter Tool operating at 400 W, $5x10^{-3}$ mbar, and 40 °C. SEM images in figure A-1 show very large grain sizes similar to the films deposited at 0.2 nm/s in the Evatek evaporator system.

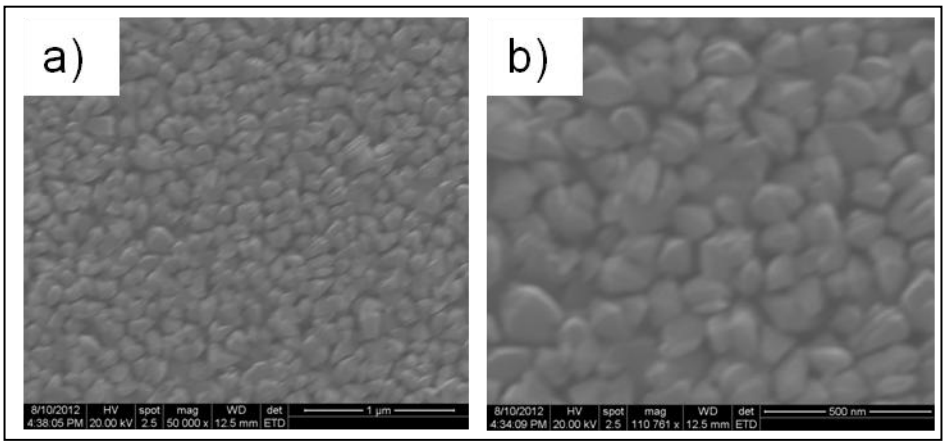

Figure A-1. SEM images with (a) 1000- and (b) 500-nm scale bars of 500-nm-thick Ti films deposited by DC magnetron sputtering.

INTENTIONALLY LEFT BLANK.

Appendix B. SEM Analysis of Pillar Cross Section

Figure B-1 shows the cross-sectional image of the 0.05 nm/s Ti film with a 300-nm diameter pillar on top of the Ti. This cross section was produced by cleaving the wafer with a diamond scribe through the patterned Si nanopillar region.

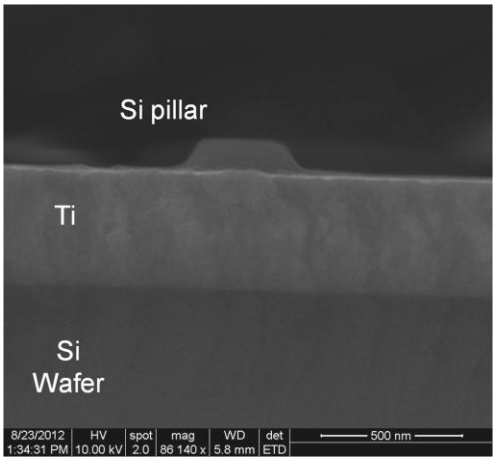

Figure B-1. SEM cross section of a 300-nm-diameter Si nanopillar on a Ti film deposited at 0.05 nm/s on a Si wafer.

INTENTIONALLY LEFT BLANK.

List of Symbols, Abbreviations, and Acronyms

AFM	atomic force microscopy
DI	deionized
FIB	focused ion beam
FWHM	full width at half maximum
HMDS	hexamethyldisilazane
IPA	isopropyl alcohol
MIBK	methyl isobutyl ketone
PMMA	poly(methyl methacrylate)
Pt	platinum
RMS	root mean square
SEM	scanning electron microscopy
Si	silicon
Ti	titanium

1 (PDF only) DEFENSE TECHNICAL INFORMATION CTR
DTIC OCA
8725 JOHN J KINGMAN RD
STE 0944
FORT BELVOIR VA 22060-6218

1 DIRECTOR
US ARMY RESEARCH LAB
IMAL HRA
2800 POWDER MILL RD
ADELPHI MD 20783-1197

1 DIRECTOR
US ARMY RESEARCH LAB
RDRL CIO LL
2800 POWDER MILL RD
ADELPHI MD 20783-1197

1 DIRECTOR
US ARMY RESEARCH LAB
RDRL CIO LT
2800 POWDER MILL RD
ADELPHI MD 20783-1197

5 US ARMY RSRCH LAB
RDRL SED C C LUNDGREN
RDRL SED C C BECKER
RDRL SEG M ROY
RDRL SEG N STRNAD
RDRL SEG W BENARD
ADELPHI MD 20783-1197

2 US ARMY RSRCH LAB
KEN STRAWHECKER
4600 DEER CREEK LOOP, L118
ABERDEEN PROVING GROUND, MD 21005-5069